Electronic Supplementary Material (ESI) for Journal of Materials Chemistry A.

Supporting Information

Graphene-based Electrochemical Filter for Water Purification

Yanbiao Liu,[a,b] Juen Hon Dustin Lee,[a] Qing Xia,[a] Ying Ma,[b] Yang Yu,[a] Lin Yue Lanry Yung,[c] Jianping Xie,[c] Choon Nam Ong,[b] Chad D. Vecitis[d] and Zhi Zhou[a,b,$,]*

[a]. Department of Civil and Environmental Engineering, Faculty of Engineering, National University of Singapore, 1 Engineering Drive 2, E1A-07-03,Singapore 117576

[b]. NUS Environmental Research Institute, National University of Singapore, 5A Engineering Drive 1, #02-01, Singapore 117411

[c]. Department of Chemical and Biomolecular Engineering, National University of Singapore, Singapore 117585

[d]. School of Engineering and Applied Sciences, Harvard University, Cambridge, Massachusetts, United States 02138

[$]. Present address: School of Civil Engineering and Division of Environmental and Ecological Engineering, Purdue University, 550 Stadium Mall Drive, West Lafayette, Indiana, United States 47907.

[*]Corresponding author: Phone: (765) 496-3559. E-mail: zhizhou@purdue.edu

Supporting information:

17 pages, 23 figures, 2 tables

Materials and Methods

Liquid chromatography-mass spectrometry (LC-MS).

A liquid chromatography-mass spectrometry (LC-MS) analysis was performed on an Agilent 1290 UHPLC system (Waldbronn, Germany) coupled to 6540 quadrupole-time of flight (Q-TOF) mass detector equipped with a dual jet stream electrospray ionization source and a MassHunter workstation. The column used for the separation was an Agilent rapid resolution HT zorbax SB-C18 (2.1 × 50 mm, 1.8 µm). The oven temperature was maintained at 35°C and the gradient elution involved a mobile phase consisting of (A) 0.1% formic acid in water and (B) 0.1% formic acid in acetonitrile. The following solvent gradient was applied: from 11% (B) to 15% (B) between 1.01 – 3.30 min; from 15% (B) to 32% (B) between 3.31 – 5.00 min; and then back to initial conditions between 5.01 – 5.50 min. Flow rate was set at 0.4 mL min-1 and 5 µL of samples was injected. The electrospray ionization-mass spectrometry (ESI-MS) was acquired in positive ion mode and the ion spray voltage and nozzle voltage was set at 4,000 V and 1,000 V, respectively. The nebulizer nitrogen gas flow rate was set at 55 psi. For a full scan mode analysis spectra were stored from m/z 50 to 500 in centroid mode.

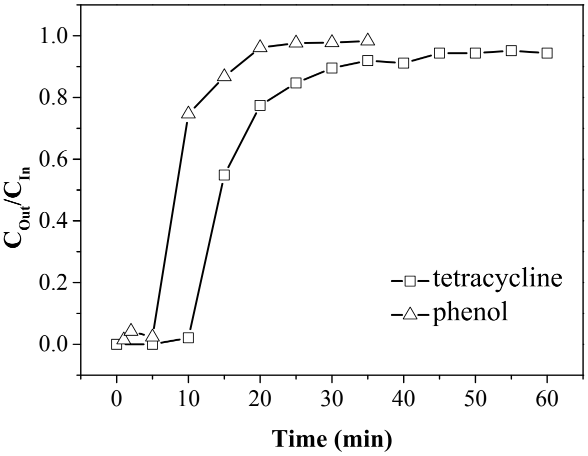

Figure S1 Breakthrough curves of 0.1 mmol L^{-1} tetracycline and 0.53 mmol L^{-1} phenol.

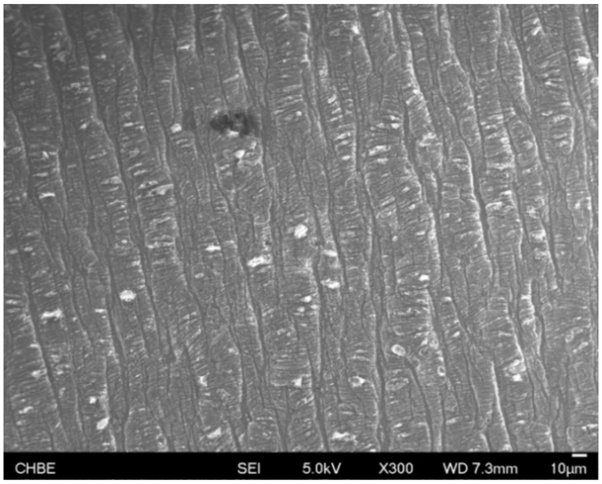

Figure S2. SEM image of a graphene filter (GNP:CNT=70%:30%) showing membrane corrugation.

Figure S3. FESEM characterization of pure GNP membrane.

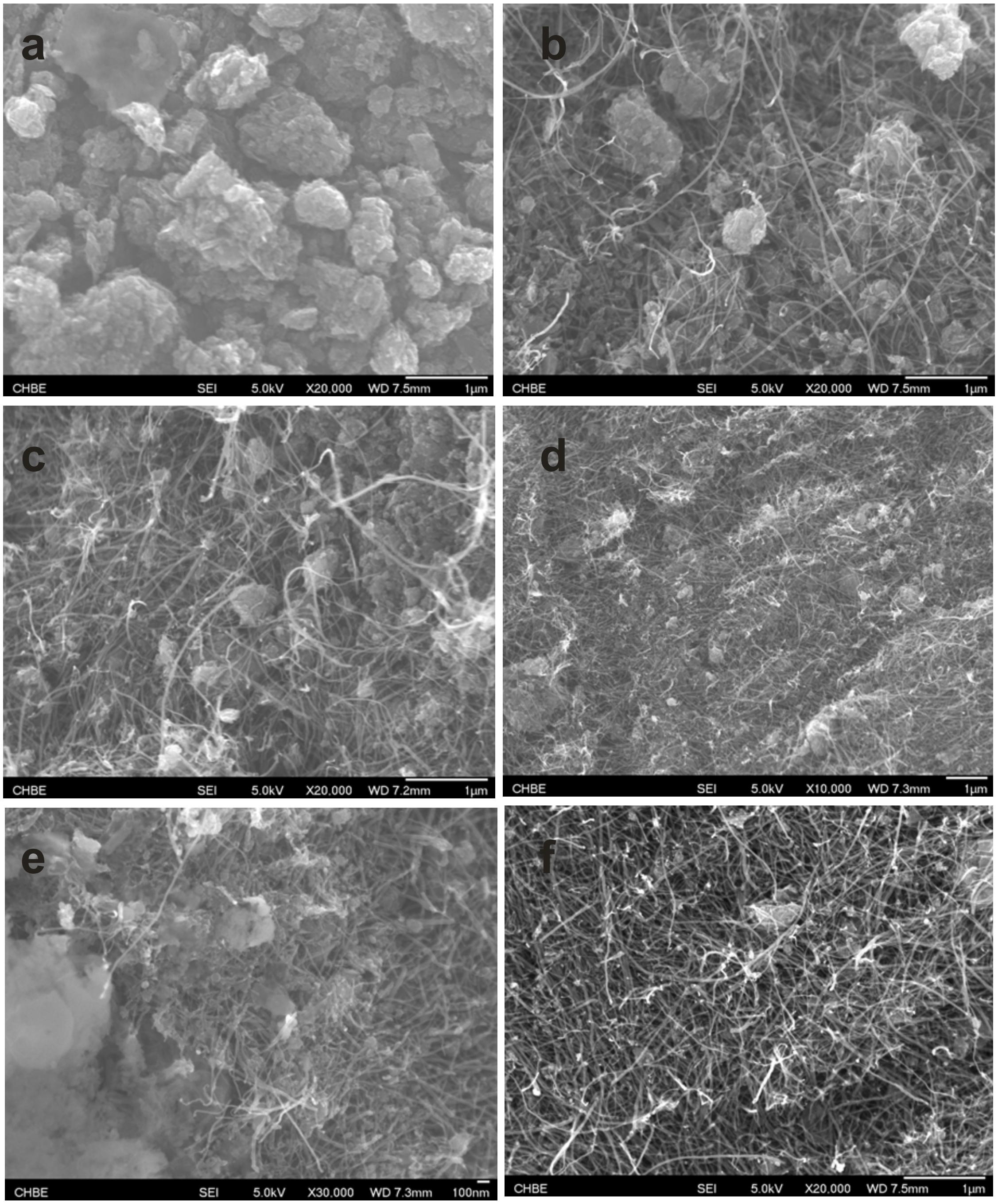

Figure S4. FESEM images of grapheme filters with different GNP:CNT ratios. (a) GNP:CNT=100%:0%; (b) GNP:CNT=90%:10%; (c) GNP:CNT=80%:20%; (d) GNP:CNT=70%:30%; (e) GNP:CNT=60%:40%; (f) GNP:CNT=50%:50%.

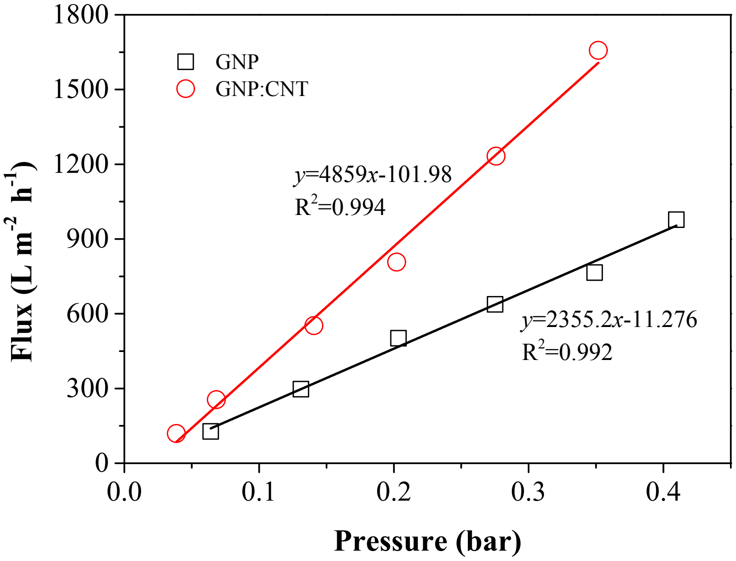

Figure S5. Water flux versus applied pressure: comparison between pure GNP membrane and 70%GNP:30%CNT membrane.

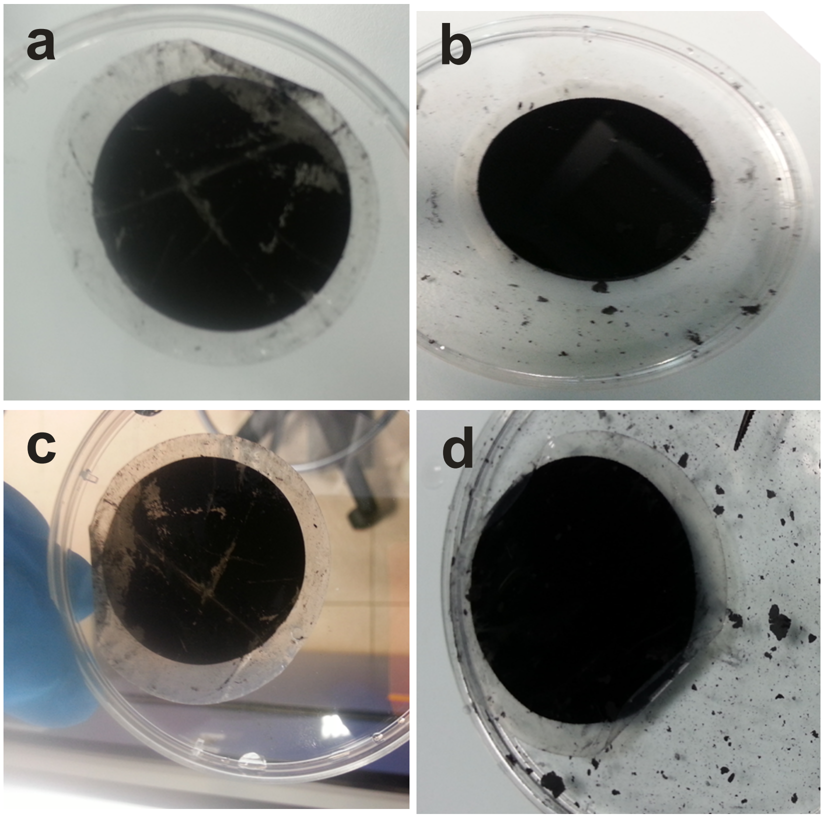

Figure S6. Images showing easily flaked off GNPs after dispersion in (a) DI-H_2O, (b) ethanol, (c) dimethyl sulfoxide, and (d) n-methyl-2-pyrrolidone.

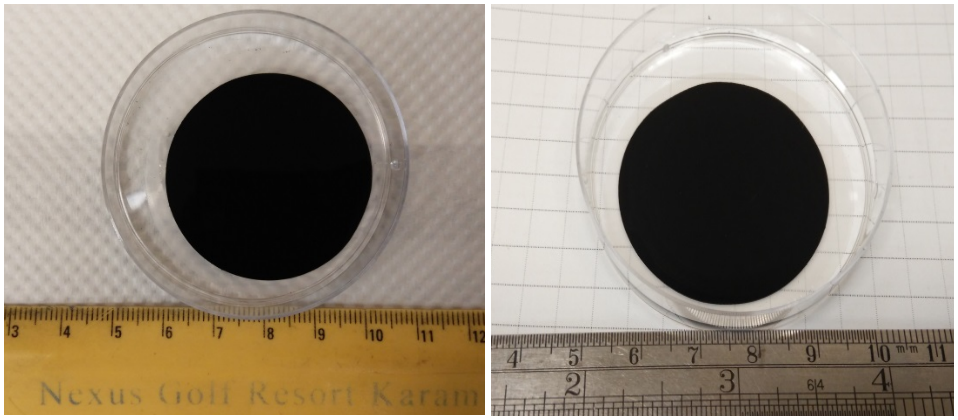

Figure S7. The digital images of the GNP-CNT filter before (A) and after (B) 2h continuous filtration of 0.1 mmol L^{-1} tetracycline, and no obvious change in physical morphology was observed.

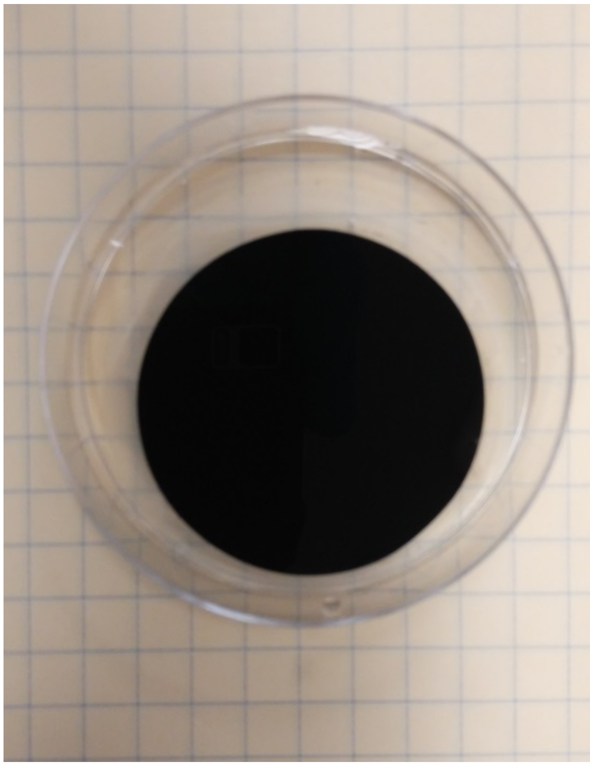

Figure S8. The digital image of a GNP-CNT filter after soaking into DI for one month and no peeling off of graphene membrane was observed, indicating a strong binding of GNP-CNT layer to the PTFE membrane.

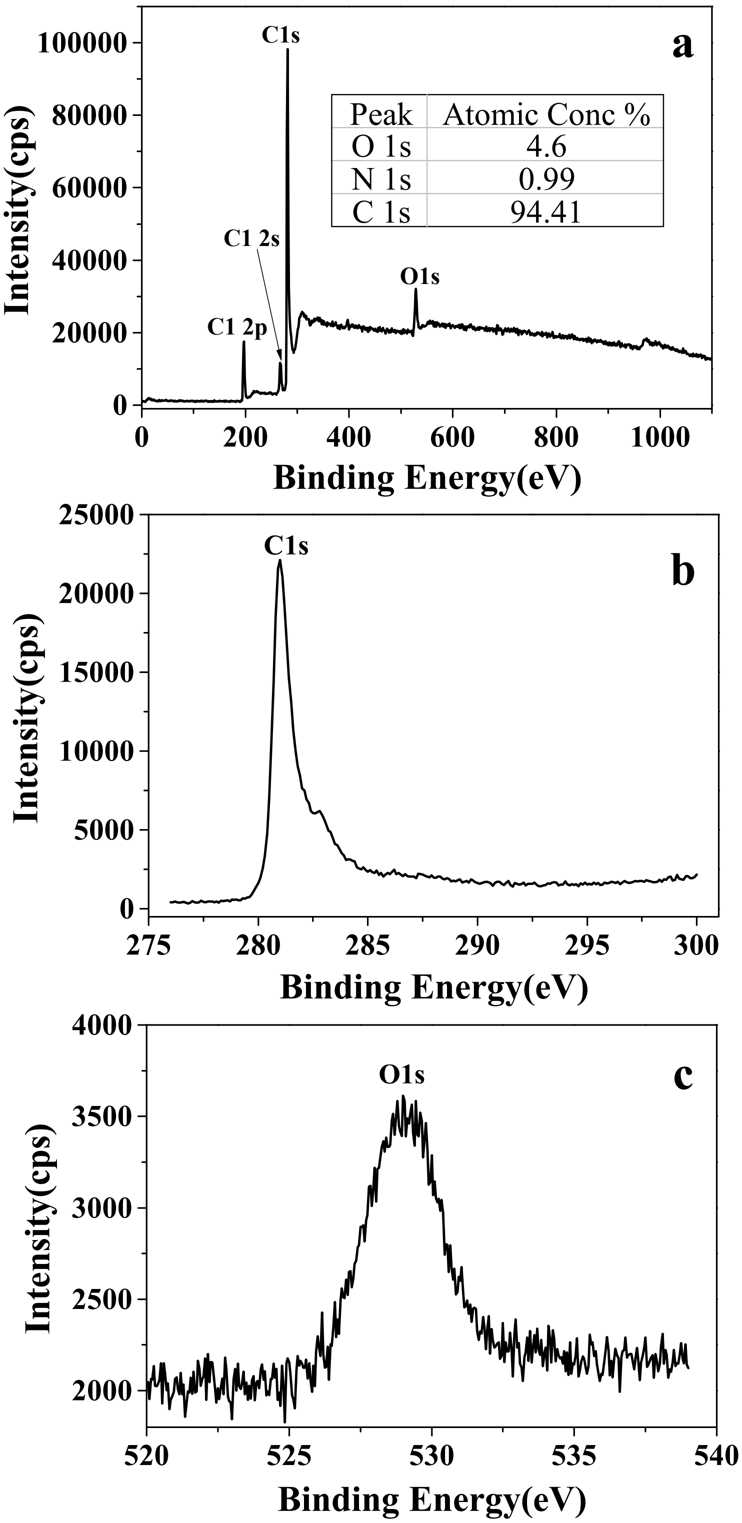

Peak	Atomic Conc %
O 1s	4.6
N 1s	0.99
C 1s	94.41

Figure S9. The XPS survey (a), C 1s (b) and O 1s (c) spectra of the GNP.

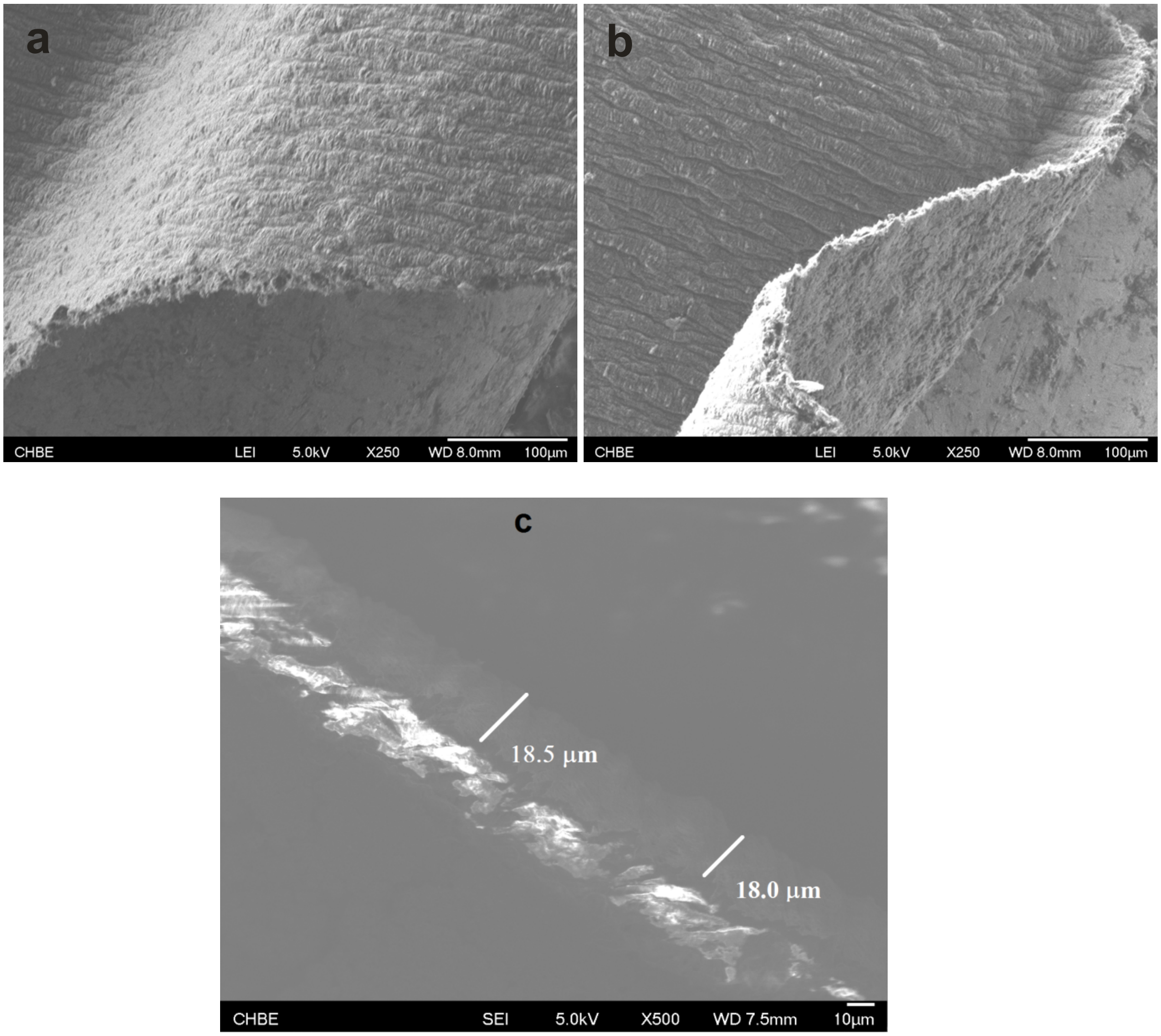

Figure S10. SEM images of the cross-sectional view of the GNP:CNT filter (a,b) and pure GNP filter (c), indicating the average membrane thickness was 15~20 µm.

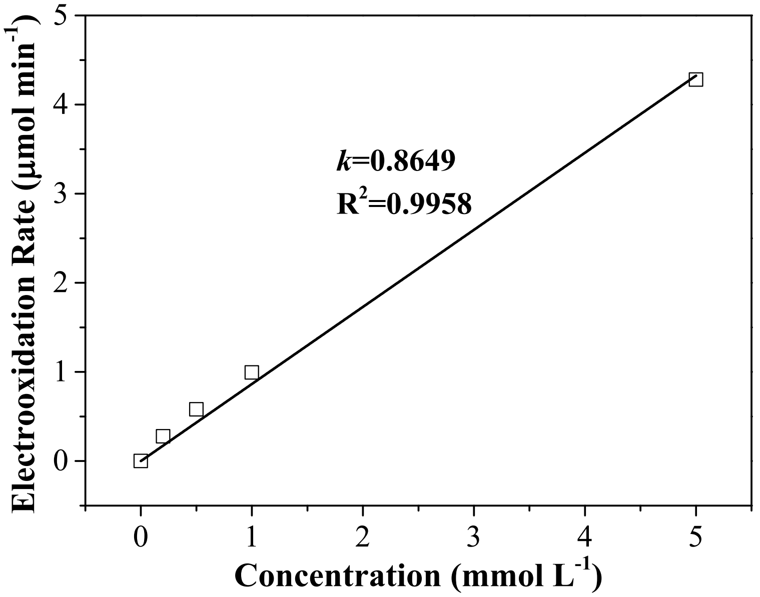

Figure S11. Correlation of oxidation rates and influent concentrations during the electrochemical filtration of ferrocyanide at 0.4 V (vs. Ag/AgCl).

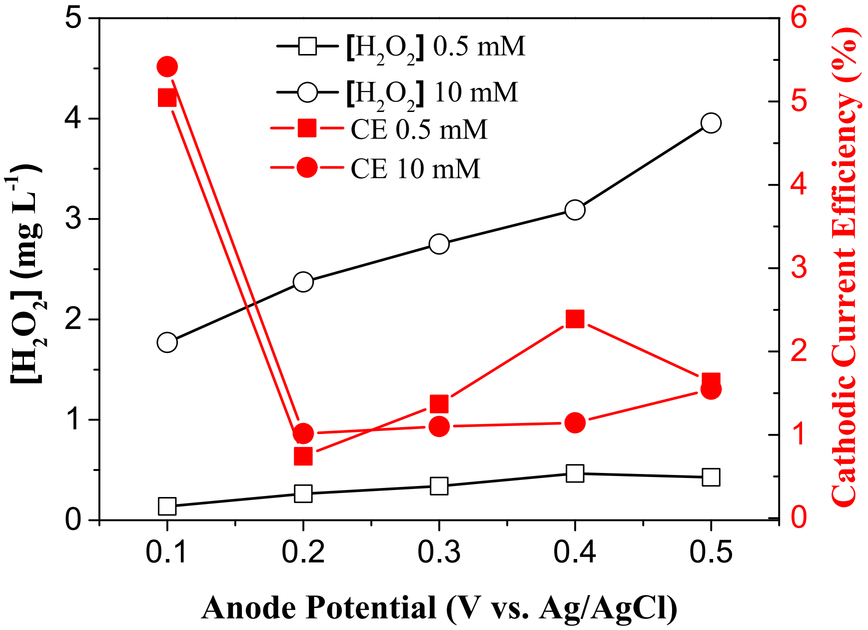

Figure S12. Effects of influent concentrations and applied potentials on H_2O_2 production and cathodic efficiency. Experimental conditions: Na_2SO_4: 10 mmol L^{-1}, flow rate: 1.5 mL min^{-1}, GNP:CNT=70%:30%.

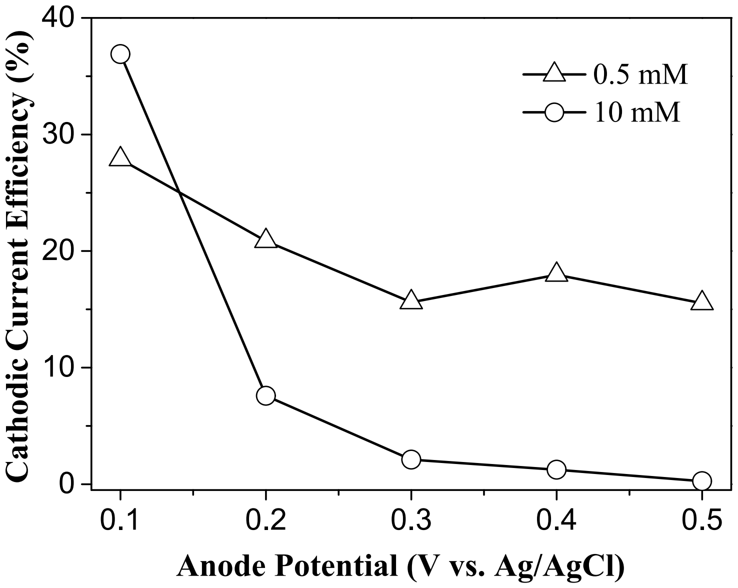

Figure S13. Effects of influent concentrations and applied potentials on the cathodic efficiency of eq. 4 ($\frac{1}{4}O_2 + \frac{1}{2}H_2O + e^- \rightarrow OH^-$).

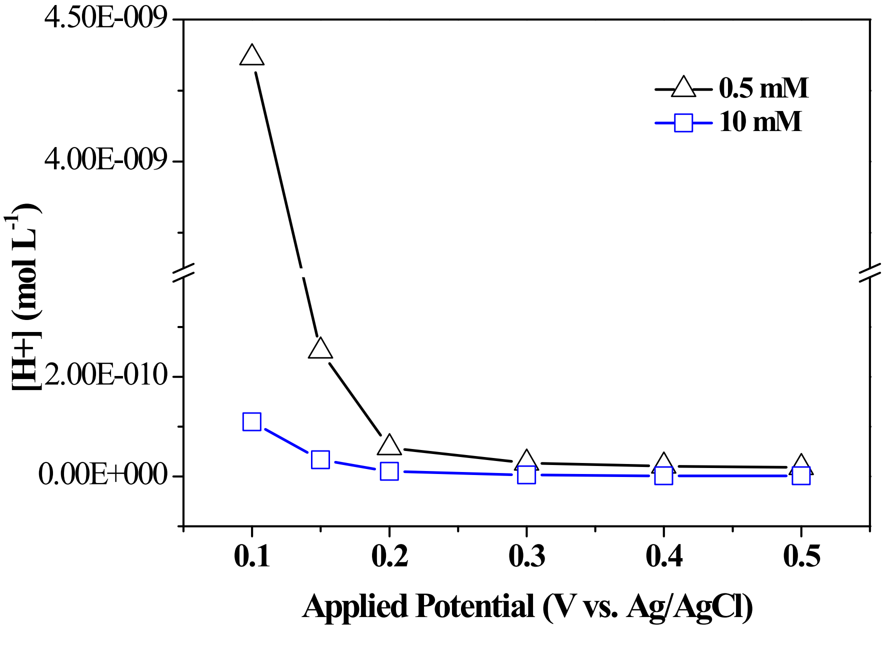

Figure S14. Effects of influent concentrations and applied potentials on proton concentration. Experimental conditions: Na_2SO_4: 10 mmol L^{-1}, flow rate: 1.5 mL min^{-1}, GNP:CNT=70%:30%.

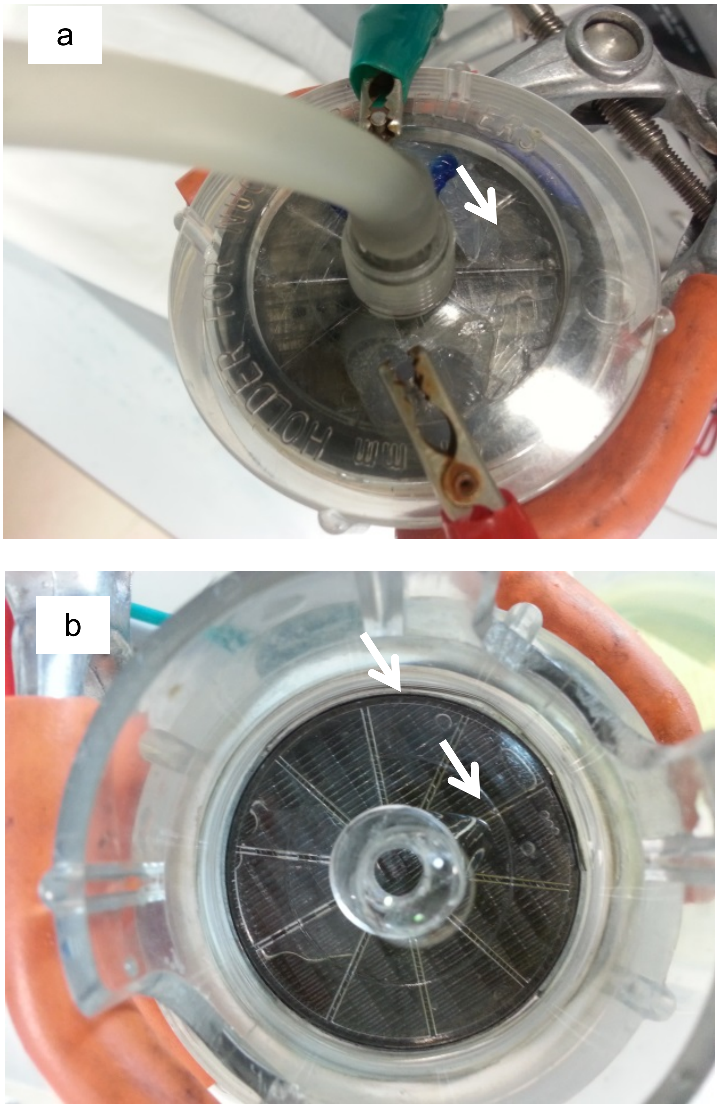

Figure S15. Formation of gas bubbles in the (a) top and (b) bottom of the filtration device duing the oxidation of ferrocyanide at 0.4 V (vs. Ag/AgCl). Arrows indicate the bubbles formed during electrichemical filtration.

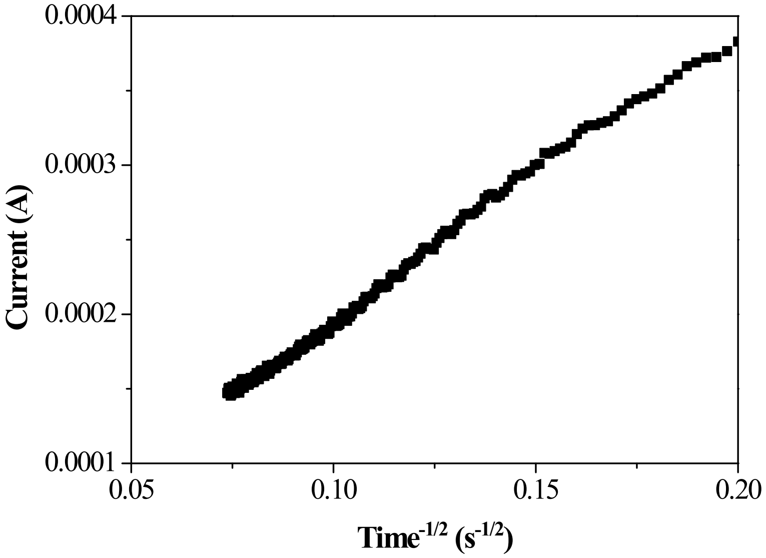

Figure S16. Plot of current and time$^{-1/2}$ for the batch system based on *Cottrell* equation.

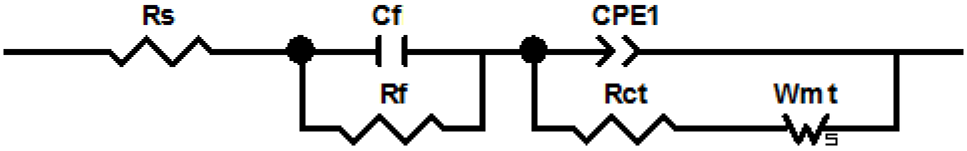

Figure S17. Equivalent circuit for the EIS spectra.

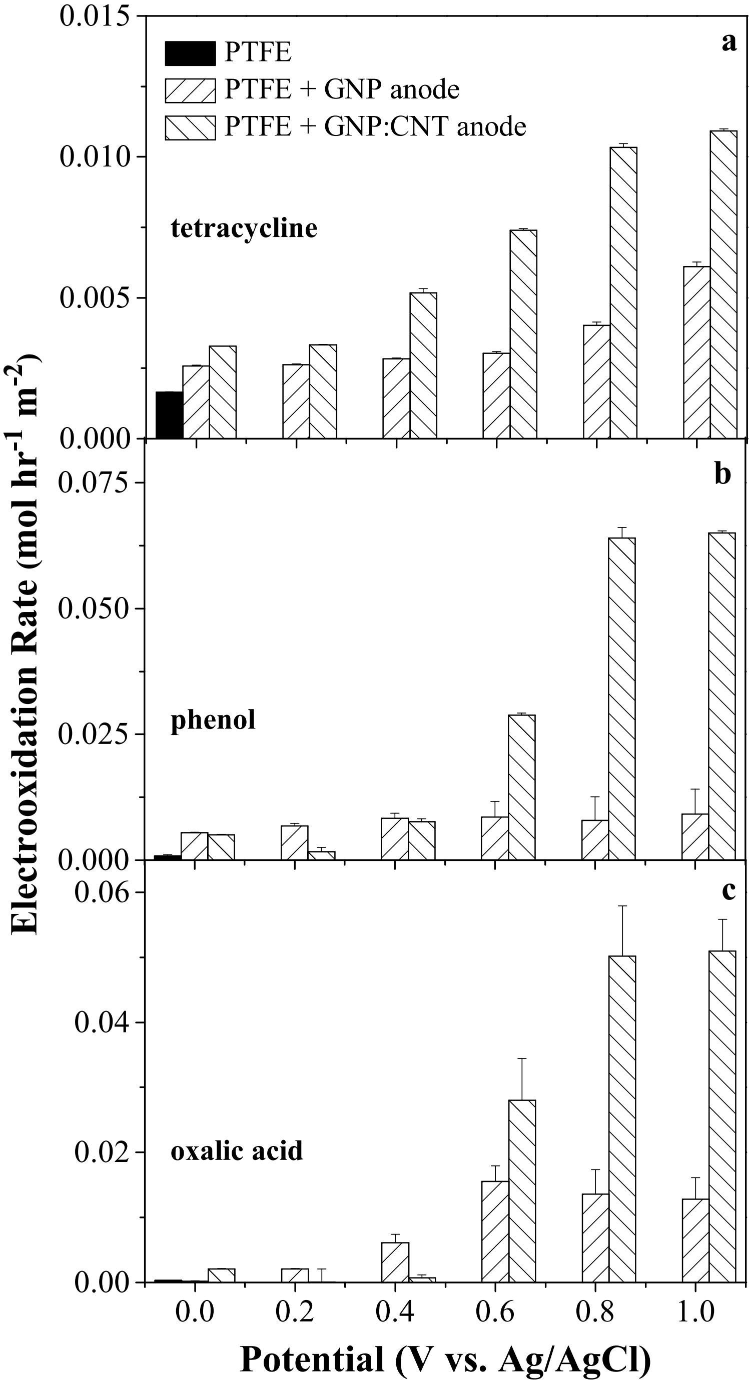

Figure S18. Effects of anodic compositions and applied potentials on electrooxidation of (a) tetracycline, (b) phenol, and (c) oxalic acid. Experimental conditions: Na_2SO_4: 10 mmol L^{-1}, flow rate: 1.5 mL min^{-1}, tetracycline: 0.1 mmol L^{-1} (26 mg C L^{-1}), phenol: 0.53 mmol L^{-1} (38 mg C L^{-1}), oxalic acid: 0.56 mmol L^{-1} (13 mg C L^{-1}). Note that there is no potential applied at conditions of 0.0 V (vs. Ag/AgCl) for all experiments.

min^{-1}.

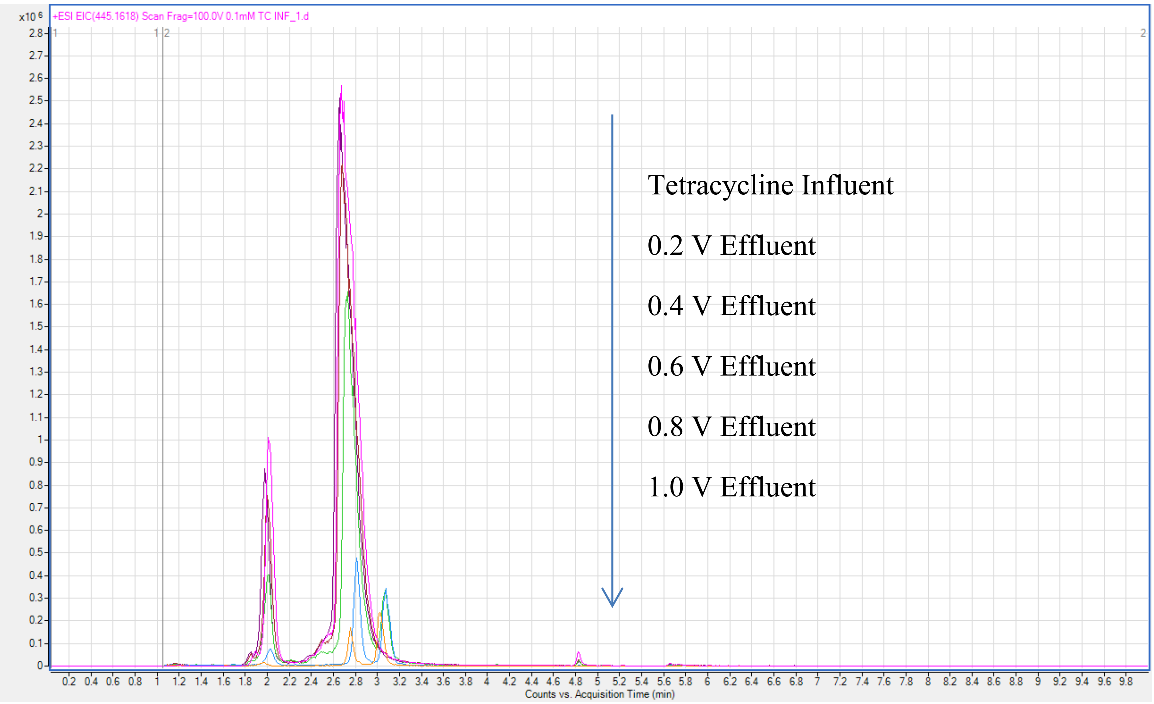

Figure S19. The extracted ion chromatogram of m/z 445.16175 of the influent tetracycline and effluent samples. Applied potential ranged from 0.2 to 1.0 V (vs. Ag/AgCl). Experimental conditions: [tetracycline]$_{\text{influent}}$: 0.1 mmol L^{-1}, Na_2SO_4: 10 mmol L^{-1}, flow rate: 1.5 mL min^{-1}.

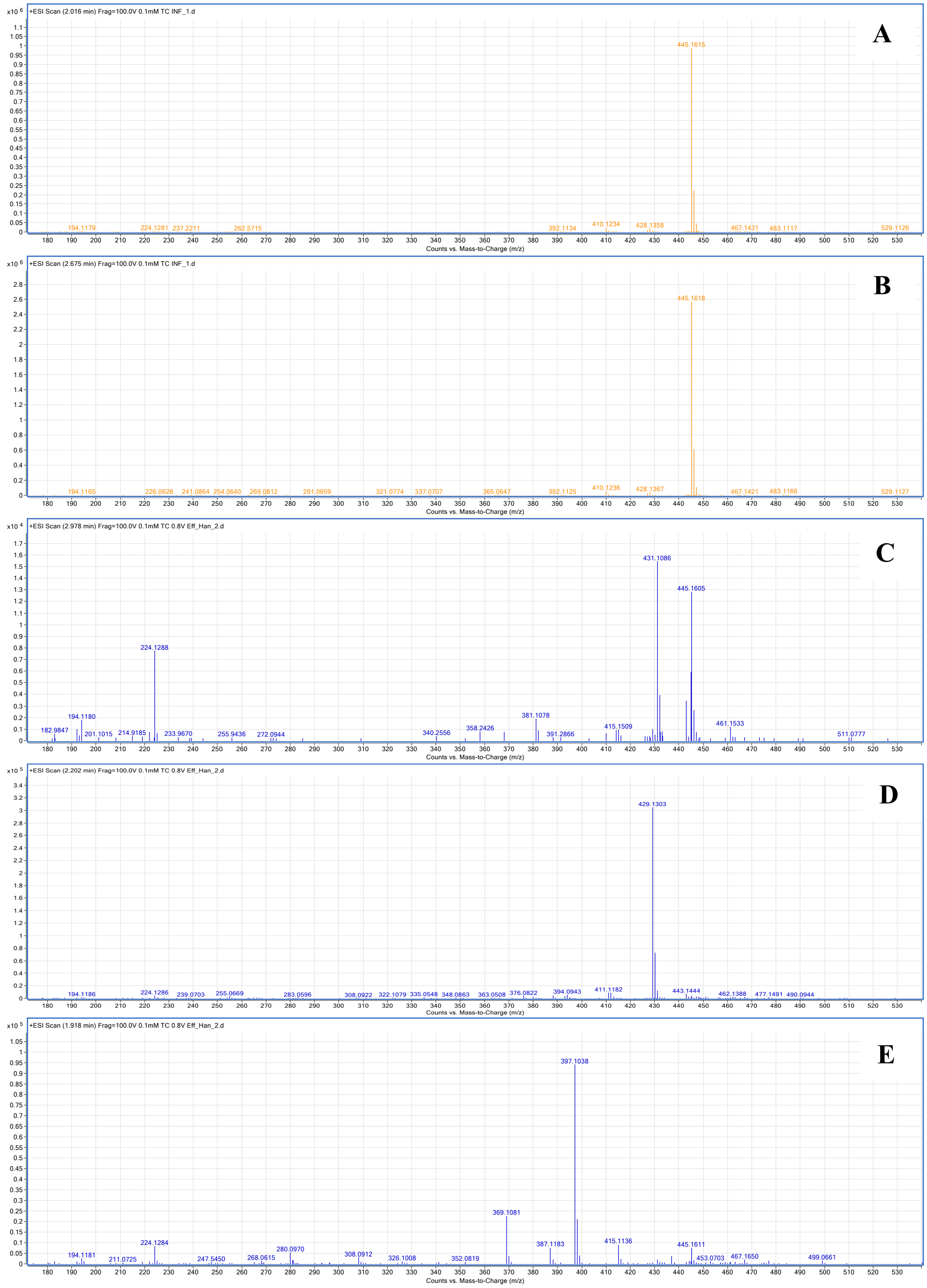

Figure S20. The MS spectra of (**A**) m/z 445.16175 (RT=2.016 min), (**B**) m/z 445.16175 (RT=2.675 min), (**C**) m/z 431.1086 (RT=2.978 min), (**D**) m/z 429.1303 (RT=2.202 min) and (**E**) m/z 397.1038 (RT=1.918 min). Experimental conditions: applied potential: 0.8 V (vs. Ag/AgCl), $[\text{tetracycline}]_{\text{influent}}$: 0.1 mmol L^{-1}, Na_2SO_4: 10 mmol L^{-1}, flow rate: 1.5 mL min^{-1}.

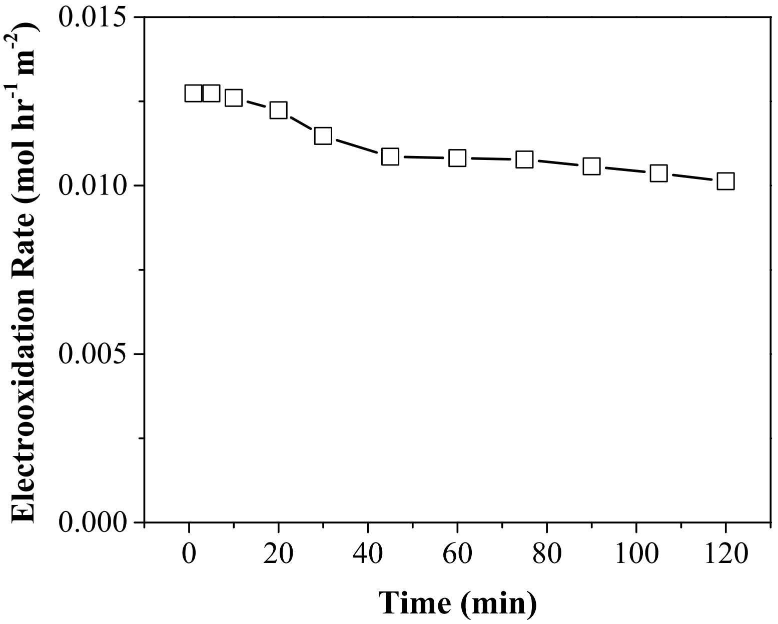

Figure S21. Tetracycline electrooxidation flux as a function of time. Experimental conditions: [tetracycline]$_{\text{influent}}$: 0.1 mmol L^{-1}, Na_2SO_4: 10 mmol L^{-1}, applied potential: 0.8 V (vs. Ag/AgCl), flow rate: 1.5 mL

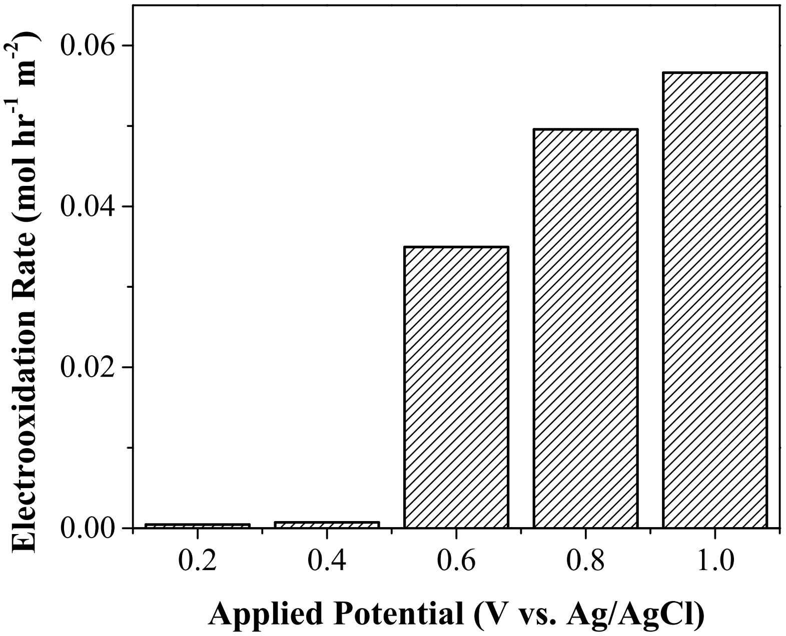

Figure S22. Electrooxidation of phenol spiked reservoir water as a function of applied potential. Experimental conditions: [phenol]$_{\text{influent}}$: 0.53 mmol L^{-1}, Na_2SO_4: 10 mmol L^{-1}, flow rate: 1.5 mL min^{-1}.

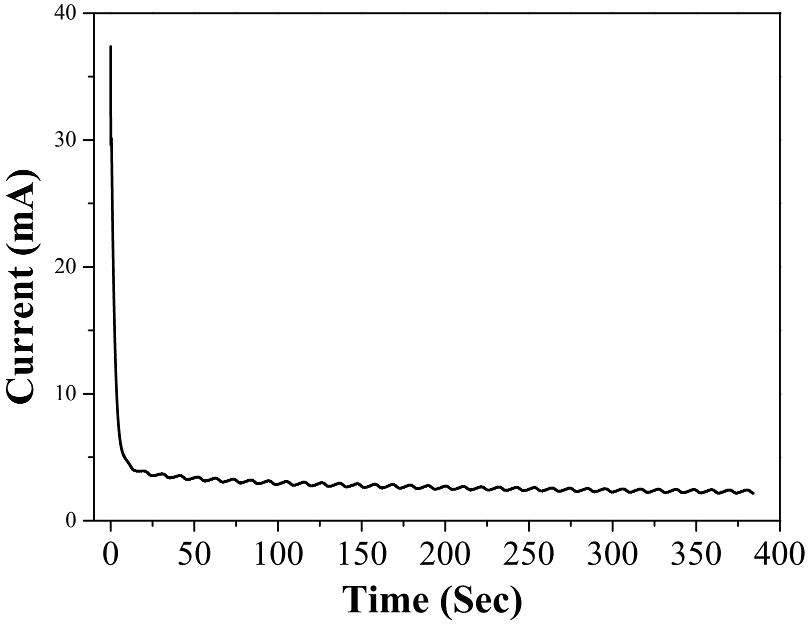

Figure S23. Current-time profile of the electrochemical GNP:CNT filter at an applied anode potential of 0.8 V (vs. Ag/AgCl). Experimental conditions: $[\text{Phenol}]_{\text{in}}$: 0.53 mmol L^{-1}, Na_2SO_4: 10 mmol L^{-1}, flow rate: 1.5 mL min^{-1}, GNP:CNT=70%:30%.

Table S1. Simulated EIS resistance and capacitance values.

System	R_s (Ω)	C_f (μF)	R_f (Ω)	CPE_{dl} (μF)	R_{ct} (Ω)	W_{mt} (Ω)
Filtration	4.093	0.219	97.73	250.0	130.0	33.5
Batch	1.312	0.136	94.10	3597.0	12.0	4.5

Table S2. Chemical characteristics of the reservoir water sample.

Parameters	Values
pH	7.25
Dissolved oxygen (mg L^{-1})	9.79
Conductivity (μS/cm)	269
Total organic carbon (mg L^{-1})	4.11